Indian J. Phys. **83** (**4**) 455-463 (2009)

Intergranular percolation in granular YBCO/$BaTiO_3$ composites

Annapurna Mohanta[1], Dhrubananda Behera[1]*, Simanchalo Panigrahi[1]
and
Naresh Chandra Mishra[2]

[1]Department of Physics, National Institute of Technology, Rourkela-769 008, Orissa, India
[2]Department of Physics, Utkal University, Bhubaneswar-751 004, Orissa, India

E-mail : dhrubananda_behera@yahoo.co.in

Abstract : Ferroelectrics and high temperature superconductors are two promising materials for future electronic devices. Both being perovskite ceramic structures with similar crystal chemistry a set of samples were prepared from the composite of (1-*x*)$YBa_2Cu_30_{7-\delta}$ – (*x*)$BaTiO_3$ (YBCO/BT). These samples were investigated with temperature dependent resistance, FTIR, X-ray diffraction and SEM-EDX analysis. It has been found that the critical exponent in the T_{c0} (R = 0) region is in agreement with the percolation theory. A long-range superconducting order results from thermally assisted percolation process through weak-links between the grains. The connectivity in the coherent transition region can be explained by a power law.

Keywords : Composite, superconductivity, percolation.

PACS Nos. : 74.81.Bd, 74.62.Dh, 74.72.Bk

1. Introduction

The perovskite ferroelectric (Ba, Sr) TiO_3 and perovskite YBCO superconductor possess similar lattice structure (2–3% lattice match in *a-b* planes) and crystal chemistry. Thus a composite of (1-*x*)YBCO – (*x*) $BaTiO_3$ provides an ideal system for experimental study. Kahiberga *et al* [1] have prepared (1-*x*)YBCO – (*x*) $BaTiO_3$ ($0 < x < 0.12$) composite and showed different Ba-containing phases (Y_2BaCuO_5, $BaCuO_2$ and CuO, Cu_2O) up to 10 wt.% in phase formation and texture analysis. Romano *et al* [2] have prepared composite of 5 wt.% $BaTiO_3$ in YBCO and explained enhanced dislocation density and strains in the YBCO matrix as a cause for larger values of J_c and strong pinning behavior in the composite. Ferroelectric material embedded in HTSC have been shown to generate a stress field and can therefore act as pinning centers [3,4].

*Corresponding Author

The mesoscopic inhomogeneities such as grain boundaries, cracks, voids *etc*. having much larger length-scale than the superconducting coherence length ξ and being temperature independent are expected to influence the *R-T* characteristics. These inhomogeneities dominate the region where zero resistance state is approached. The microscopic inhomogeneities such as structural (twin boundaries, stacking faults) and chemical imperfections (oxygen deficiencies *etc*.) inside the grains occur in a length-scale smaller than the mesoscopic inhomogeneities, but still larger than ξ. The nature of the superconducting transition, particularly the region just above and below T_c is strongly influenced by the intra and inter-granular characteristics respectively. Temperature dependent resistivity of the composite system depends on the connectivity of the grains.

In this paper we suggest that long-range superconducting order results from a thermally assisted percolation process through the weak-links between the grains. The connectivity in the coherent transition region can be explained by a power law.

2. Experimental

YBCO was prepared from the stoichiometric amounts of high-purity powders of Y_2O_3, $BaCO_3$, and CuO and $BaTiO_3$ has been prepared by solid state reaction method by mixing $BaCO_3$ and TiO_2 in a calculated proportion sintered at 1300°C for eight hours. Superconductor YBCO-ferroelectric $BaTiO_3$ composites were made from a mixture of pre-reacted YBCO powder and $BaTiO_3$ powder. A series of polycrystalline composite samples of (1-*x*) YBCO – (*x*) $BaTiO_3$ (where x = 1.0, 2.5, 5.0 and 10.0) have been prepared by the standard solid-state reaction method. Pressed composite pellets were sintered at 900°C for 12 h and then cooled to 500°C, where they were kept for 12 h in an oxygen atmosphere for oxygen annealing.

All the samples were characterized by X-ray powder diffraction technique (PW 3020 vertical goniometer and 3710 X'Pert MPD control unit, CuK_α), and temperature dependent resistance was measured using standard four-probe method with a nanovoltmeter (Keithley-181) and an indigenously developed constant current source. The grain morphology of the samples was analyzed by scanning electron microscopy (Model No JSM-6480 LV, Make JEOL). Compositional analysis was determined by energy dispersive X-ray analysis (EDX) using an INCA Oxford analyzer attached to a scanning electron microscope.

3. Results and discussion

3.1. Phase formation :

The XRD patterns (Figure 1) of YBCO/$BaTiO_3$ samples were indexed and found to be in the orthorhombic phase at room temperature with a space group P_{mmm}. The lattice parameters and unit cell volumes of the samples are obtained using chekcell software

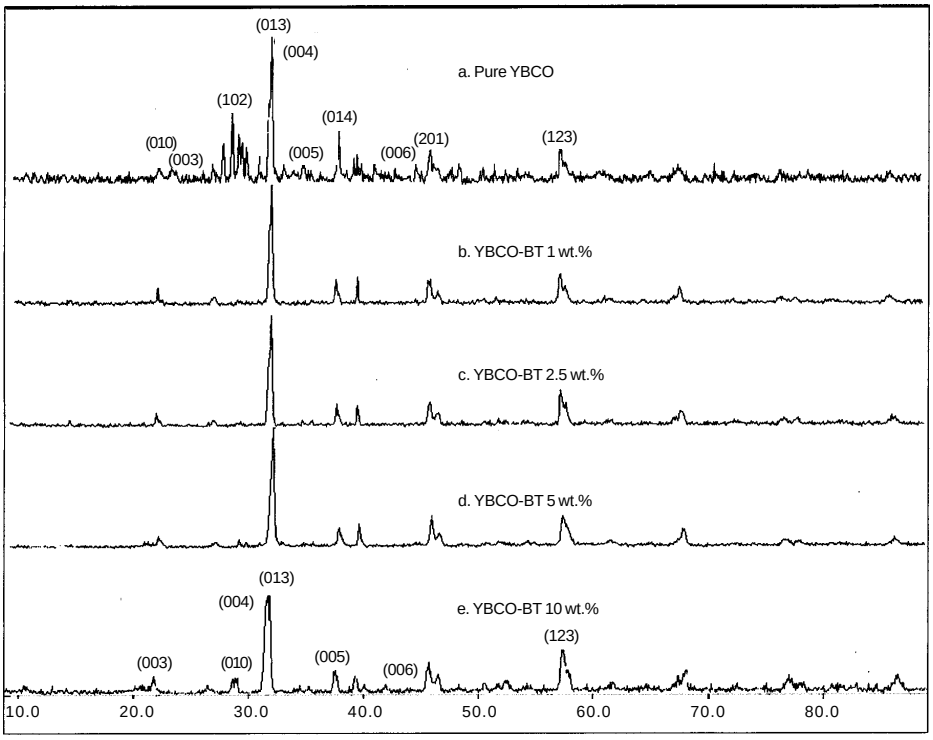

Figure 1. XRD patterns of (a) YBCO, (b) YBCO-BT 1 wt.%, (c) YBCO-BT 2.5 wt.%, (d) YBCO- BT 5 wt.% and (e) YBCO-BT 10 wt.%.

and presented in Table 1. It is found that the lattice parameters (*a*, *b* and *c*) are in agreement with those published for undoped YBCO [5]. Appearance of peaks (003), (004), (005) and (006) in the XRD pattern indicate that the composites have certain grain alignment in *c*-axis (Figures 1 and 2). The XRD patterns of composite system showed no noticeable impurity peaks. However, in 10 wt.% $BaTiO_3$ tiny peaks with corresponding intensity at $2\theta = 30°$ and peak at (110) increases in the XRD spectrum. The transition of phase from orthorhombic to tetragonal can occur if some amount of Ti goes into lattice site in the composite of YBCO and BT where BT is expected to reside at the grain boundary. Here all the samples are found to be orthorhombic without

Table 1. Lattice parameters and unit cell volumes of the samples, pure YBCO, YBCO-1 wt.% BT, YBCO-2.5 wt.% BT, YBCO-5 wt.% BT and YBCO-10 % wt.% BT.

BT wt.%	*a*(Å)	*b*(Å)	*c*(Å)	Volume (Å)
0	3.8273	3.8882	11.6369	173.9015
1.0	3.7881	3.8771	11.6344	171.6069
2.5	3.8296	3.8860	11.6874	173.9298
5.0	3.8338	3.8862	11.7180	174.5854
10.0	3.8226	3.8799	11.7090	173.6597

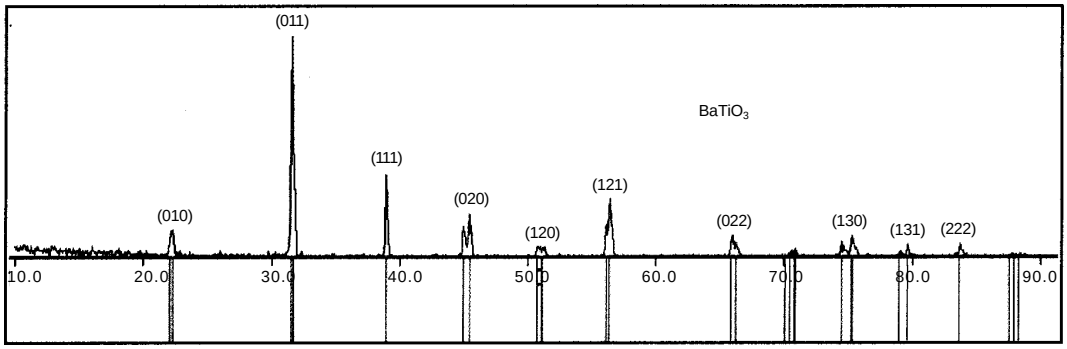

Figure 2. XRD patterns of $BaTiO_3$ sample.

any signature of phase transition. This problem is analogous to our previous study in YBCO/Ag composite, where Ag diffuses into the grains [6].

The average size of the crystallites (t) in the composites was estimated from XRD pattern using Scherrer's equation

$$t = K\lambda/\beta \cos \theta$$

where K is Scherrer constant, λ is the wavelength of radiation, β is the full width at half maximum in radians and θ is the corresponding angle of the peak position; this is shown in Table 2. If we neglet 10 wt.% BT composite, it can be observed from Table 2 that the crystallite sizes are almost same (0.1 μm < t < 0.2 μm).

Table 2. Orthorhombic distortion (δ), variation of othorhombicity, particle size (t) of pure YBCO, YBCO-1 wt.% BT, YBCO-2.5 wt.% BT, YBCO-5.0 wt.% BT and YBCO-10.0 wt.% BT samples.

BT wt.%	Orthorhombic distortion (δ)	Variation of orthorhombicity	Crystallite size (t) in μm
0	0.0158	0.0159	0.1765
1.0	0.0232	0.0234	0.1640
2.5	0.0146	0.0147	0.1304
5.0	0.0135	0.0136	0.1978
10.0	0.0148	0.0149	0.0760

The variation of orthorhombicity = $(b–a)/a$ and orthorhombic distortion $\delta = 2(b - a)/(b + a)$ decreases in the low concentrations while it shows a slight variation from the actual behavior in case of maximum BT 10 wt.%. According to Jorgenson *et al* [7] the decrease in orthorhombic distortion indicates the increase of oxygen vacancy in CuO chain. The structure of YBCO is basically dictated by oxygen ordering [7–9]. The above result on structural changes due to the presence of $BaTiO_3$ is due to the oxygen vacancy ordering in the system.

Figure 3 shows the lattice parameters of each sample obtained from chekcell

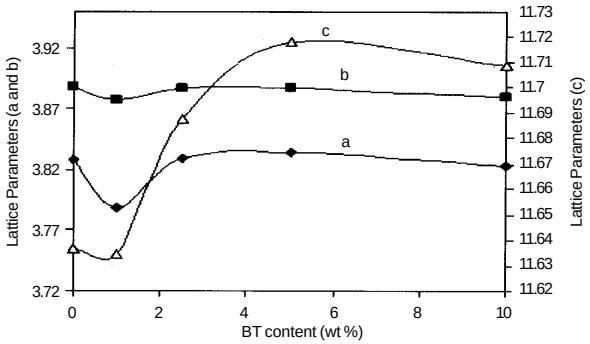

Figure 3. Variation of lattice parameters in the composite system.

software. All the lattice parameters, *a*, *b* and *c* decreased in 1 wt.% BT composite from that of YBCO may be due to the difference in radii between YBCO and BT molecules. This difference in radii results in a shrinkage of the perovskite layer in the structure. It may be noticed from the Table 1 that the parameters *a*, *b* and *c* increase with further increasing BT wt.% in the composites but for maximum concentration *i.e*. for $BaTiO_3$ with 10 wt.%, the values slightly decrease. This behaviour is due to the oxygen vacancy ordering in the composite system.

FTIR was found to be by far the most sensitive technique to identify minimal $BaCO_3$ in which the quantity as small as 0.1 wt.% was still able to be detected. It is known that absorption peaks in FTIR spectrum, which appears below 800 up to 400 cm^{-1} are caused by different kinds of metal oxygen bonds present in the sample. The observed intense peak at 1429 cm^{-1} (Figure 4) is probably due to carbonate bond bonded with Ba ions [10]. Around 1700 cm^{-1} another bond appears which assigned to

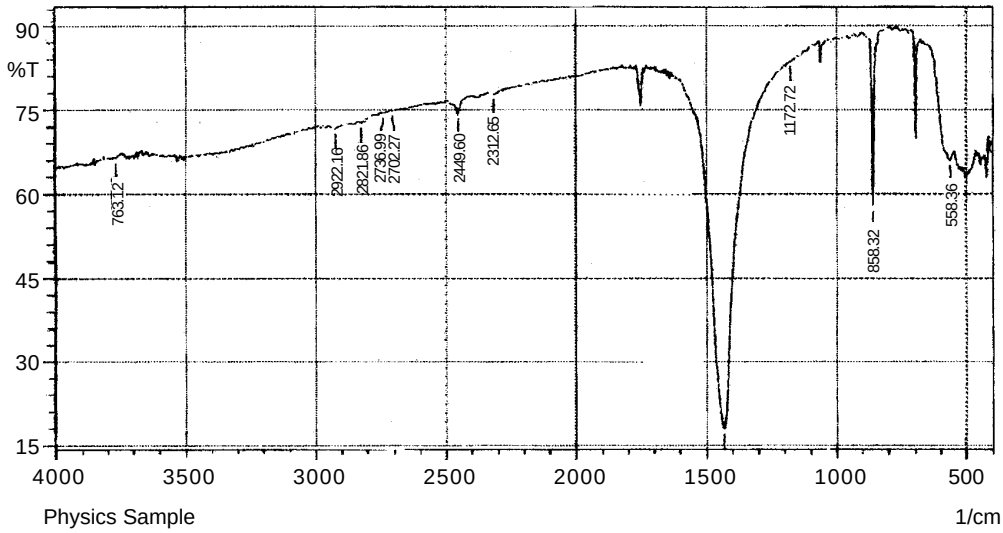

Figure 4. FTIR of YBCO-$BaTiO_3$ composite sample.

the C=O stretching mode [11]. FTIR peaks at 858 cm^{-1} are identified as $BaTiO_3$ phase. This shows that BT has separate phase in the composite as has been identified by XRD spectrum.

The scanning electron microscopic (SEM) images of the prepared samples are presented in Figure 5. It is observed from the SEM results that the grain sizes are almost same and nearly 10 to 20 crystallites are expected to be present in a grain of YBCO/BT composite. It is believed that the Ti-ions concentrate near the grain boundaries which substantially reduce grain mobility and when the boundary moves, adsorbs the impurities.

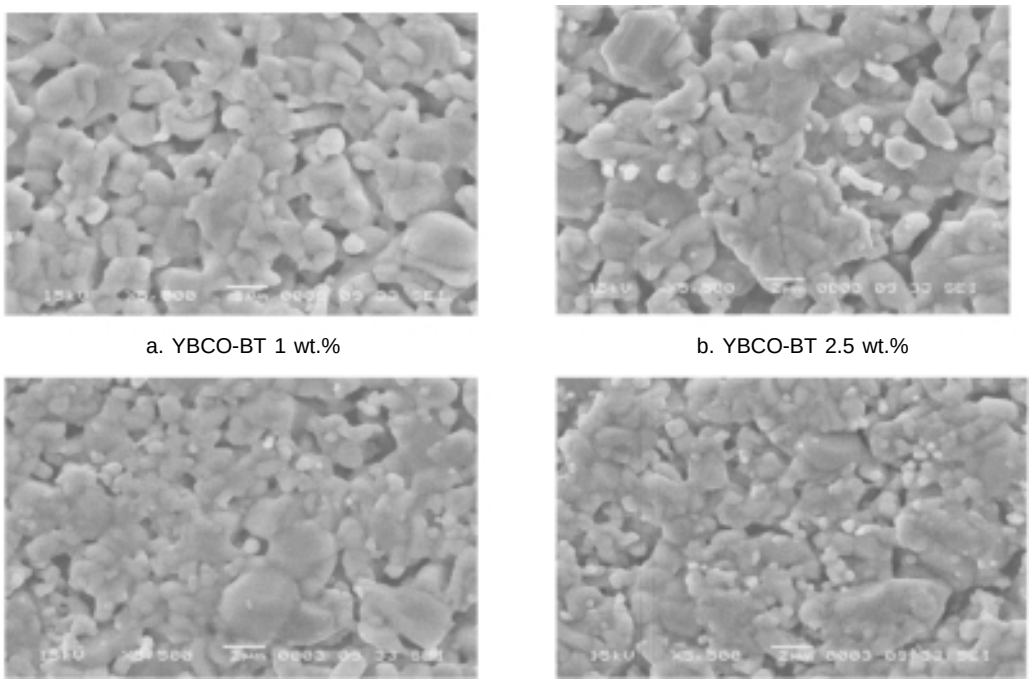

a. YBCO-BT 1 wt.% b. YBCO-BT 2.5 wt.%

c. YBCO-BT 5 wt.% d. YBCO-BT 10 wt.%

Figure 5. SEM images of (a) YBCO-BT 1 wt.%, (b) YBCO- BT 2.5 wt.%, (c) YBCO- BT 5 wt.% and (d) YBCO-BT 10 wt.%.

3.2. Microstructure-dependent resistance variation with temperature :

The temperature dependence of normalized resistance for composite samples of (1-*x*)YBCO – (*x*) $BaTiO_3$ is shown in Figure 5. Here the resistance value is normalized with respect to that of room temperature. It is observed that metallic phase crosses over to semiconducting before being superconducting for higher concentration of BT. Onset transition temperature T_c does not decrease for the composites under the study. However, a large variation in T_{c0} (R = 0) occurs here. T_{c0} decreases from 84.8 K to 72.7 K with increasing $BaTiO_3$ from 0 to 10 wt.%. At lower temperature, where the

intergrain coupling energy exceeds the thermal energy, global phase ordering occurs and the sample enters the zero-dissipation state. In the temperature interval between T_c and T_{c0} , excess conductivity occurs and the resistivity is expected to exhibit a highly non-ohmic behavior. As a result of composite formation T_c is not affected for low concentration (within 10 wt.%). However for 10 wt.% of the composite, a small decrease in T_c (~1 K) is observed. It is clear from the *R-T* graphs (Figure 6) that with increasing BT concentration, the resistance of the samples increases significantly. In YBCO-BT system the resistance increases due to insulating BT particles which effectively reduces the number of superconducting paths.

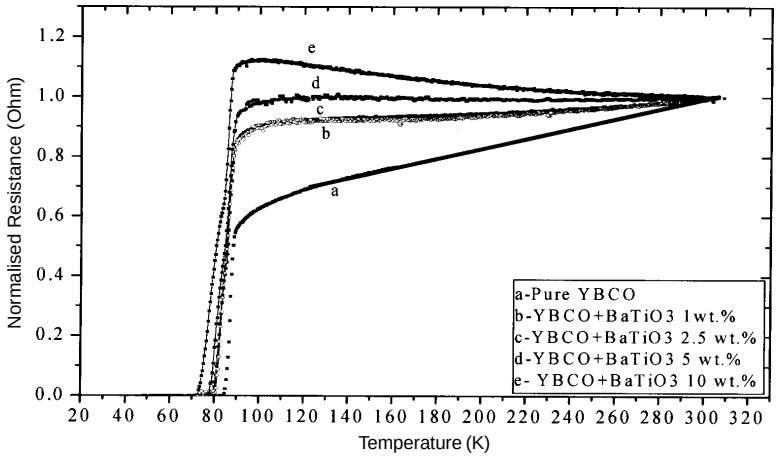

Figure 6. Temperature dependent resistance in YBCO + $BaTiO_3$ composites with different wt.%.

A finite tailing at the lower end of the superconducting transition has been shown in Figure 6 for all the YBCO/$BaTiO_3$ composite samples before the resistance attains zero value. The zero-resistance at the temperature T_{c0}, characterizes the onset of global superconductivity in the samples where the long-range superconducting order is achieved. The approach to this state in the form of tailing indicates that the superconducting grains get progressively coupled to each other by Josephson tunneling across the grain boundary weak links. This type of tailing feature in the resistive transition close to T_{c0} has been seen mostly in granular superconductors.

3.3. Approach to zero-resistance state :

In the tailing region close to T_{c0}, this heterogeneous medium consists of two components. For the first component the superconducting grains and the grain boundary weak links has been considered through which superconductivity is established through Josephson tunneling. The second component consists of weak links which are not superconducting, either due to the link being too weak or due to the measuring current of the corresponding link or the temperature being higher than the T_c of that link. For $T < T_{c0}$, the first component provides the channel for the transport of

supercurrent. For $T_{c0} < T < T_c$, the volume of the first component is not adequate enough to provide a percolative path for supercurrent and the *R*-*T* transition shows a tail with $R \neq 0$. Only when $T \leq T_{c0}$, a percolative path through the first component is established and a global superconductivity is achieved in the sample with *R* going to zero.

In the temperature close to T_{c0}, attempts has been made to fit the resistance to a power law of the form

$$R = A\varepsilon_0^{\delta}$$

where, ε_0 is the reduced temperature, $T - T_{c0}/T_{c0}$ and δ is the exponent.

The apparent universality of δ (~1.33) from Figure 7, the exponent is a consequence of purely geometrical factor of the current percolation. A more adequate interpretation is perhaps to suppose that percolation is accompanied by a genuine thermodynamic transition [12], where long range order is established among the superconducting grains as the phase of the order parameter locks collectively. In this model, superconducting fluctuations across the inter-grain junctions are responsible for the power law behavior. The regime of approach to the zero resistance state reveals the occurrence of a coherence transition at a lower temperature T_{c0}.

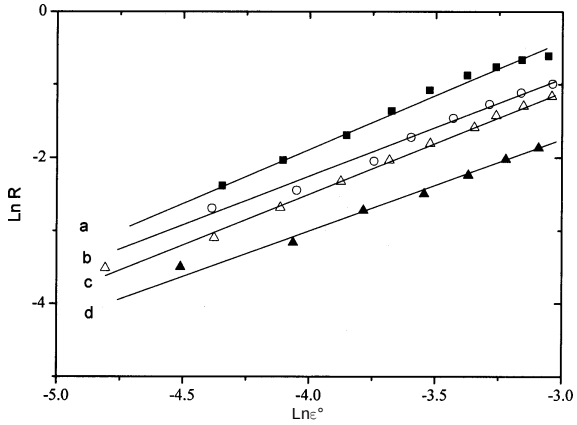

Figure 7. Logarithmic plot of resistance as function of reduced temperature ($\varepsilon_0 = T - T_{c0}/T_{c0}$) where T_{c0} is the temperature at zero resistance for YBCO + BT(*a* = 0, *b* = 1, *c* = 2.5, *d* = 10 wt.%).

4. Conclusion

Close to the zero-resistance temperature a power law regime is found, with the same exponent in all compositions. For this second transition (T_{c0}), we estimate that the transport critical exponent, δ = 1.33 is in agreement with the percolation theory. It shows a behavior approaching the exponent of three-dimensional percolation model. The lattice parameters from XRD data reveal that there is no diffusion of Ti ions into the YBCO and it is a result of better composite formation. The observation of weak interfacial reactivity is confirmed by SEM and FTIR. This gives strong evidence that

transport in the composites takes place in 3D and indirectly confirms that the interfacial reactivity between the two materials is very weak. This suggests that long-range superconducting order results from a thermally assisted percolation process through the weak-links between the grains.

References

[1] M Kahiberga, M Livinsh, M Kundzinsh, A Sternberg, I Shorubalko, L Shebanovs and K Bormanis *J. Low Tem. Phys.* **105** 1433 (1996)

[2] L T Romano, O F Schilling and C R M Grovmor *Physica* **C178** 41 (1991)

[3] O F Schilling *Appl. Phys. Lett.* **52** 1817 (1988)

[4] W Gawalek, T Habisreuther, K Fischer, G Bruchlos and P G Qrnert *Cryogenics* **33** 65 (1993)

[5] Morsy Abou Sekkina, Abdul Raouf Tawfik, Osama Hemeda, Mohamad Ahmad Taher Dawoud and Samy El-attar *Turk. J. Phys.* **29** 329 (2005)

[6] D Behera and N C Mishra *Supercond. Sci. Technol.* **15** 72 (2002)

[7] J D Jorgensen, B W Veal, A P Paulikjs, L J Lowicki and G W Grabtree *Phys. Rev.* **B41** 1863 (1990)

[8] N C Mishra, A K Rajarajan, K Patnaik, R Vijayaraghavan and L C Gupta *Solid State Commun.* **75** 987 (1990)

[9] A Porch, J R Cooper, D N Zheng, J R Waldram, A M Campbell and P A Freeman *Physica* **C214** 350 (1993)

[10] M M Silvan, L F Cobas, R J M-Palma, M H Velez and J M M-Duart *Surf. Coat Technol.* **151** 118 (2002)

[11] P Duran, D Gutierrez, J Tataj, M A Banares and C Moure *J. Eur. Ceram. Soc.* **22** 797 (2002)

[12] P Pureur, J Schaf, M A Gusmao and J V Kunzler *Physica* **C176** 357 (1991)